# Optimizing Smart Home Microgrid Through Demand Response Based On Mamdani Fuzzy Inference System

**Christelle Arielle Mbouteu Megaptche[1], Sebastian Waita[1], Peter Moses Musau[2] and Bernard Odhiambo Aduda[1]**

1 Department of Physics, University of Nairobi, Nairobi P.O. Box 30197-00100 (Kenya)

2 Department of Electrical Electronic and Information Engineering, South Eastern Kenya University, Kitui P.O. Box 170-90200 (Kenya)

## Abstract

This study presents the development and implementation of a demand response-based energy management strategy using a Mamdani Fuzzy Inference System (FIS) within a smart home microgrid powered by hybrid renewable energy sources in Garoua, Cameroon. The system integrates photovoltaic (PV), wind turbine (WT), and battery storage components, whose optimal configuration was determined using Particle Swarm Optimization (PSO) to minimize the Levelized Cost of Energy (LCOE). A fuzzy logic controller dynamically manages energy flow and prioritizes controllable household loads based on five real-time inputs: PV output, WT output, battery state of charge (SoC), electricity consumption, and time of day. Simulation results demonstrate a reduction in energy consumption by 8.675%, enhanced utilization of renewable resources, and 15.0676% energy export to the grid, offering economic opportunities through feed-in tariffs or net metering. The proposed FIS-based demand response strategy effectively flattens load peaks, fills valleys, and improves the overall efficiency, flexibility, and resilience of the microgrid without compromising user comfort.

*Keywords: Smart home microgrid, Demand response, Fuzzy inference system, Energy optimization, Renewable energy integration.*

## 1. Introduction

Fuzzy logic is increasingly integrated into residential energy management systems to enhance demand response (DR) strategies by optimizing energy use and improving customer comfort. Incentive-based DR programs aim to reduce peak-hour consumption by shifting loads to off-peak periods. Acun & Çunkaş (2023) introduced an economical fuzzy logic-controlled home energy management system for real-time energy regulation in households. The controller acquires inputs from sensors and modulates lighting, heating, and cooling output power based on sensor data and user demands. This technology efficiently decreases total household energy usage while maintaining user comfort, making it a critical and user-friendly element of home energy management systems. Ain et al. (2018) introduced a Fuzzy Inference System (FIS) to manage smart buildings' home energy. The FIS uses humidity as a variable to adjust thermostat set points dynamically, hence improving user comfort. It also reduces indoor temperature variations by offering feedback for enhanced energy efficiency. The study presented an automated, rule-based generation and assessed the system utilizing Mamdani FIS and Sugeno FIS, demonstrating a 28% reduction in energy use. Similarly, Paramathma et al. (2021) introduced a fuzzy logic-based method for smart home load management, reallocating electricity use to off-peak periods. The system accounted for pricing, time, and user preferences to optimize cost, efficiency, and comfort, while enabling seamless demand response participation.

More advanced systems have emerged, such as the type-2 fuzzy controllers by Beheshtikhoo et al. (2023), which developed them for smart homes integrating renewables and electric vehicles. Their system reduced grid electricity use by 343.95 kWh weekly, cut costs by 71.5%, and lowered the peak-to-average ratio by 64.6%, highlighting its effectiveness for sustainable energy management. Javaid et al. (2023) proposed a fuzzy deep neural optimizer for seasonal energy scheduling in smart homes. It improved energy efficiency and cost reduction across seasons, outperforming previous models. The study also highlighted key challenges, including power forecasting, multi-objective optimization, and integration with cloud computing and microgrids. Finally, Žarković & Dobrić (2019) proposed a fuzzy expert system for managing smart hybrid energy microgrids. The system enhances energy consumption and storage efficiency, boosting microgrid profitability through renewable energy sources. The system's decisions concerning energy production, controllable loads, and consumption are guided by input factors like insolation, energy pricing, temperature, wind speed, and load


10.18086/swc.2025.07.08 Available at http://proceedings.ises.org

power.

While existing studies have demonstrated the potential of fuzzy logic controllers in optimizing residential energy consumption, most focus on either individual appliance control, simplified demand response scenarios, or idealized system simulations without integrating comprehensive microgrid elements. Furthermore, limited research has addressed the coordinated control of multiple energy sources, such as solar and wind, alongside storage systems and user comfort constraints in a unified framework. There remains a need for a practical, scalable approach that incorporates real-time environmental inputs, user demand, and grid interaction into a smart microgrid system. This study addresses this gap by proposing a demand response strategy based on a Mamdani Fuzzy Inference System to intelligently manage energy flow in a hybrid renewable-powered smart home microgrid optimized using particle swarm optimization.

## 2. Methodology

This study presents the design and control of a smart home microgrid system intended for a residential setting in a residential area with high renewable potential. The proposed system integrates renewable energy sources, energy storage, and intelligent load control in a hybrid DC/AC microgrid configuration.

### *2.1. System Description*

The proposed system is implemented for a residential household in Garoua, Cameroon, with an annual electricity consumption of 3159.44 kWh. The microgrid is structured around a dual-source generation setup, combining photovoltaic and wind energy, with battery storage to enhance energy autonomy and resilience. The system is connected to household AC loads through an inverter and a hybrid bus, ensuring efficient energy distribution and conversion. The sizing of these components is optimized using Particle Swarm Optimization (PSO). To manage energy consumption and renewable energy intelligently, a Mamdani Fuzzy Inference System (FIS) is employed. It takes as inputs the energy outputs of the PV and wind systems, the battery state of charge, household energy consumption, and the time of day to dynamically optimize both energy usage and load distribution. The system prioritizes the use of renewable energy while ensuring user comfort and reliability.

### *2.2. Hybrid Renewable Energy System Optimization Approach*

A Particle Swarm Optimization (PSO) algorithm is employed to determine the optimal configuration of system components. The PSO aims to minimize the levelized cost of energy (LCOE) by selecting the most appropriate sizing of generation and storage elements. The objective function is defined as presented in eq. 1:

$$OF = Min(LCOE) \qquad \text{(eq. 1)}$$

LCOE results from the Net Present Cost (NPC) calculation. NPC represents the total lifetime cost of implementing the hybrid renewable energy system (HRES) over the project's 20-year horizon. It encompasses all relevant expenses, including initial capital investment, component replacements, operation, and maintenance. The Levelized Cost of Energy (COE), expressed in $/kWh, is derived from the NPC and reflects the average unit cost of electricity generated by the system. To ensure accurate economic evaluation, the Capital Recovery Factor (CRF) is applied to account for the time value of money. This factor enables the conversion of future costs into their present value, thereby improving the reliability of long-term financial analysis. The methodology for calculating the NPC of an HRES is outlined by Tezer et al. (2017):

$$NPC = \sum_{i=1}^{n} N_i \times \left[(CC_i + RC_i \times F_i(rir, L_i, Z_i) + OMC_i) \times CRF[rir, Y]\right] \qquad \text{(eq. 2)}$$

The components utilized in this equation are outlined as follows: $F_i$ denotes the present worth factor for component $i$, while $OMC_i$ indicates the yearly operation and maintenance cost associated with component $i$. The variable $n$ signifies the total number of components within the HRES. $N_i$ refers to the quantity of system component $i$ per unit, $CC_i$ represents the capital cost, and $RC_i$ encompasses the overall cost of replacing the component $i$ throughout the system's lifespan. Lastly, $CRF$ stands for the Capital Recovery Factor. The $CRF$ is influenced by the real interest rate ($rir$) and the project timeframe ($Y$) and can be calculated as follow:

$$CRF[rir, Y] = \frac{rir[1+ir]^Y}{[1+rir]^Y - 1} \qquad \text{(eq. 3)}$$

$$F = \sum_{n=1}^{Z_i} \frac{1}{[1+rir]^{L_i \times n}} \quad \text{(eq. 4)}$$

$Z_i$ denotes the total number of times component $i$ is replaced during the useful lifespan of project $Y$, while $L_i$ indicates the useful lifetime of that component.

Following the determination of the net present cost, the calculation of the electricity cost proceeds as outlined below (Bukar et al., 2019; Kotb et al., 2020):

$$LCOE = \frac{NPC}{Total\ useful\ energy\ served} \quad \text{(eq. 5)}$$

The optimization is subject to the following constraints represented by eq. 6, eq. 7, and eq. 8:

$$N_x^{min} \leq N_x \leq N_x^{max}, x = \{PV, WT, BT\} \quad \text{(eq. 6)}$$

$$0 \leq LPSP(Loss\ of\ Power\ Supply\ Probability) \leq 1 \quad \text{(eq. 7)}$$

With

$$LPSP = \frac{\sum_1^{8760}((P_L(t)-(P_{PV}(t)+P_{WT}(t))-(P_{BT}(t-1)-P_{BTmin}))*\eta_{inv}}{\sum_1^{8760} P_{demand}(t)} \quad \text{(eq. 8)}$$

LPSP quantifies the proportion of total energy demand that the energy system fails to meet over a given period.
In eq. 8, $P_L$ represents the load profile, $P_{PV}$ denotes the solar power production, $P_{WT}$ is the wind turbine power output, $P_{BT}$ indicates the battery power, $\eta_{inv}$ stands for the inverter efficiency, and $P_{demand}$ refers to the total power demand of the load.

The following subsections provide a comprehensive overview of how each component of the system has been modeled.

### 2.2.1. Photovoltaic Panel Generator (PV) Modeling

The hourly energy generation from the PV panels, represented as $P_{PV}$ (kW), is determined by solar insolation and environmental temperature, as outlined in eq. 9 (Bukar et al., 2019; Zaki Diab et al., 2019; Barakat et al., 2020).

$$P_{PV} = \sum_{t=1}^{8760} \left(P_{pvr} N_{pv} PV_{df}\right) \left(\frac{G(t)}{G_{base}}\right) \left(1 + K_T \left(\left(T_{amb}(t) + G(t) \times \left(\frac{NOCT-20}{800}\right) * 1000\right) - T_{base}\right)\right) \quad \text{(eq. 9)}$$

In this context, $P_{PV}$ represents the photovoltaic power output (kW), while $P_{pvr}$ is the rated output per panel, and $N_{pv}$ denotes the number of PV panels. The derating factor ($PV_{df}$) accounts for performance losses due to real-world conditions such as dust, wiring losses, and shading. $G$ is the actual solar irradiance on the tilted surface, and $G_{base}$ is the standard reference irradiance (1 kW/m² at 25°C). The power temperature effect is captured by the coefficient $K_T = -3.7 \times 10^{-3}/°C$, applied using ambient temperature ($T_{amb}$) and reference temperature ($T_{base}$), with $NOCT$ denoting the nominal cell operating temperature.

### 2.2.2. Wind Turbine (WT) Modeling

The output power of the wind generator is estimated in eq. 10 (Ramli et al., 2018):

$$P_{WT} = \begin{cases} N_{WT} \times \eta_W \times P_{WTr} \times \sum_{t=1}^{8760} \left(\frac{V(t)^3 - V_{ci}^3}{V_r^3 - V_{ci}^3}\right), & V \leq V_r \\ N_{WT} \times \eta_W \times P_{WTr}, & V_r \leq V \leq V_{co} \\ 0, & V_{co} \leq V\ or\ V \leq V_{ci} \end{cases} \quad \text{(eq. 10)}$$

Where $V$ is the recorded wind speed at hub height in meters per second (m/s) and may be calculated using eq. 11.

$$V(t) = V_{ref} \left(\frac{H_{WT}}{H_r}\right)^{\alpha} \quad \text{(eq. 11)}$$

For surfaces with negligible roughness and a wide-open site, the friction parameter $\alpha$ has a value of (1/7); the wind turbine hub height is denoted by $H_{WT}$, and the base altitude is denoted by $H_r$.

$P_{WT}$ stands for wind turbine output power (kW), $N_{WT}$ stands for the number of wind turbines, $\eta_W$ stands for wind turbine efficiency, and $P_{WTr}$ is for wind turbine calculated power (kW). $V$ is the recorded wind speed in (m/s), $V_{ci}$ is the wind speed cut in (m/s), $V_{co}$ is the wind speed termination in (m/s), $V_r$ is the rated wind speed in (m/s), and $V_{ref}$ is the estimated wind speed in (m/s).

### 2.2.3. Battery (BT) Storage System Modeling

Batteries save the extra energy system capacity to be utilized when needed (Alshammari and Asumadu, 2020). According to the authors, the following limits are applying to battery storage:

$$E_{batt,min} \leq E_{batt}(t) \leq E_{batt,max} \quad \text{(eq. 12)}$$

$$E_{batt,max} = N_{Batt}.E_{batt,cap} \quad \text{(eq. 13)}$$

$$E_{batt,min} = E_{batt,max}(1 - DOD) \quad \text{(eq. 14)}$$

Where $E_{batt,cap}$ denotes the nominal capacity of the battery bank (kWh), $E_{batt,min}$ denotes the least permissible storage battery capacity, $E_{batt,max}$ denotes the maximum allowable storage battery capacity, and $N_{Batt}$ the number of batteries. $DOD$ is the depth of discharge.

Table 1 summarizes the economic and technical aspects of the system elements (Hermann et al., 2021)

**Tab. 1: Economic and technical aspects of the HRES elements**

| Description | Parameters | Values | Units |
|---|---|---|---|
| Suntech solar panel Polycrystalline | Lifespan | 20 | Years |
| | Efficiency | 88 | % |
| | Rated power | 265 | W |
| | PV regulator cost | 450 | $/kW |
| | O&M cost | 0.01 $*$ initial cost | $/ year |
| Senwei energy Ltd. – Wind Turbine | Lifespan | 20 | Years |
| | Rated power | 2 | kW |
| | Cut-in speed | 2.5 | m/s |
| | Cut-out speed | 25 | m/s |
| | Rated wind speed | 8 | m/s |
| | Capital cost | 750 | $ per unit |
| | O&M cost | 10 | $/unit/year |
| | Hub height | 15 | m |
| | Efficiency | 96 | % |
| Surrette S-260 battery | Nominal capacity | 3.12 | kWh |
| | Roundtrip efficiency | 80 | % |
| | Maximum depth of discharge Life | 80 | % |
| | Storage bank losses | 1 | % |
| | Capital & Replacement cost | 350 | $ |
| | O&M cost | 10 | $/yr |
| | Lifespan | 12 | Years |
| Generic 1200CH - Inverter | Size | 1200 | VA |
| | Capital cost | 2000 | $ |
| | Replacement cost | 2000 | $ |
| | O&M cost | 200 | $ |
| | Efficiency | 95 | % |
| | Lifespan | 10 | Years |
| Economic parameters | Real interest | 3.5 | % |
| | Project lifetime | 20 | Years |

### 2.2.4. Converter/Inverter Modelling

Converters and inverters play a crucial role in HRES by ensuring a balanced energy flow between AC and DC devices. Converters transform power from alternating current to direct current, while inverters change direct current into alternating current. A variety of design methodologies for power converters are detailed in the current literature. This investigation utilizes the peak load methodology for the design of converters, as articulated by Ma & Javed (2019) :

$$P_{inv} = \frac{P_{peak}}{\eta_{inv}} \quad \text{(eq. 15)}$$

$P_{peak}$ denotes the system's maximum instantaneous load requirement, while $\eta_{inv}$ reflects the efficiency of the converter or inverter.

## 2.2. Energy Management Optimization using Fuzzy Inference System

To complement the component sizing results obtained from the Particle Swarm Optimization (PSO) approach, this study integrates a Mamdani-type Fuzzy Inference System (FIS) for real-time energy management in the smart home microgrid. The PSO determines the optimal system design for minimizing the Levelized Cost of Energy (LCOE), while the FIS dynamically orchestrates power flow between sources (PV, WT, battery) and household loads to improve efficiency and reduce energy wastage. The primary objective of this control mechanism is to improve energy efficiency, reduce losses, preserve battery lifespan, and enhance comfort for end users. The full control and optimization framework is illustrated in Fig.1, showing the interaction between generation sources, the FIS controller, PSO module, and household loads.

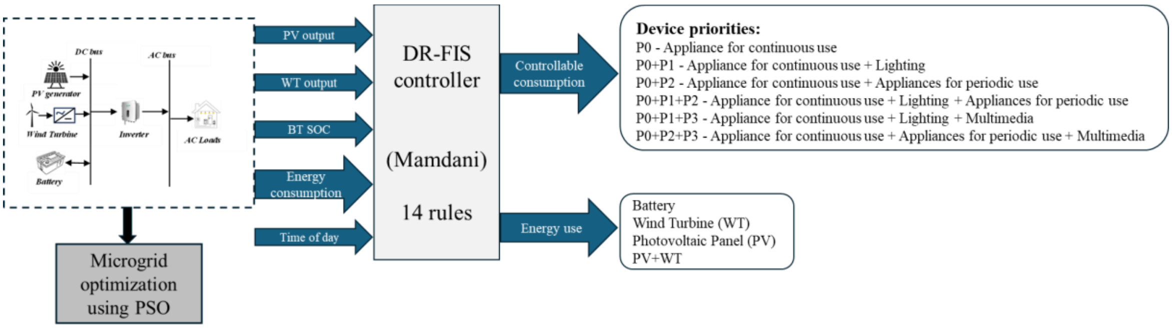


**Fig. 1: Architecture of the Smart Home Microgrid System with PSO Optimization and DR-FIS Controller**

The Fuzzy Inference System (FIS) is designed with five input variables: photovoltaic (PV) power output, wind turbine (WT) power output, battery state of charge (SoC), electricity consumption, and time of day. Based on these inputs, the controller produces two output variables: controllable consumption, which represents load scheduling decisions, and used energy, which indicates the prioritized energy source. The system was modeled and simulated in MATLAB using the Fuzzy Logic Toolbox, with 14 carefully formulated fuzzy rules. Input fuzzification is performed using triangular and trapezoidal membership functions, while defuzzification is carried out through the centroid method.

### 2.2.1. Fuzzy Inference System Design

Each input variable is linguistically categorized to represent real operating conditions. For instance, the time of day is divided into five periods: early morning, morning, afternoon, evening, and night. The photovoltaic (PV) and wind turbine (WT) power outputs are classified as low, medium, or high according to their normalized power values, while electricity consumption, ranging from 0 to 1 kW, is categorized in a similar manner. The battery state of charge (SoC) is defined in three levels: low (0-50%), medium (45-75%), and high (70-100%), to capture its dynamic operational status.

Figs 2 and 3 present the membership function for “Time of day” and “Wind Turbine output” fuzzy input variables. The time of the day membership functions are constructed using a combination of trapezoidal and triangular curves, enabling the controller to adapt to typical residential activity patterns throughout a 24-hour cycle. Similarly, the membership functions of the wind Turbine power output reflect variations in real-time wind power availability and guide the fuzzy rules toward optimal source prioritization.

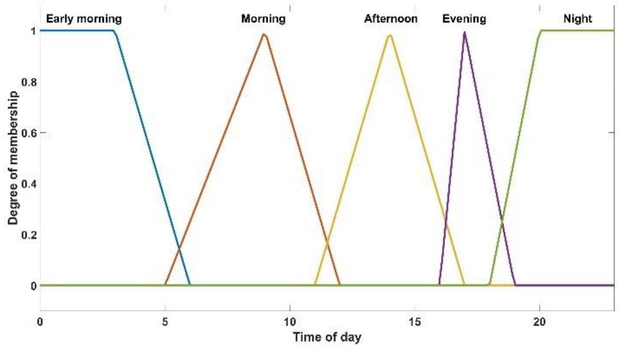


**Fig. 2: Membership function for "Time of day" fuzzy input variable**

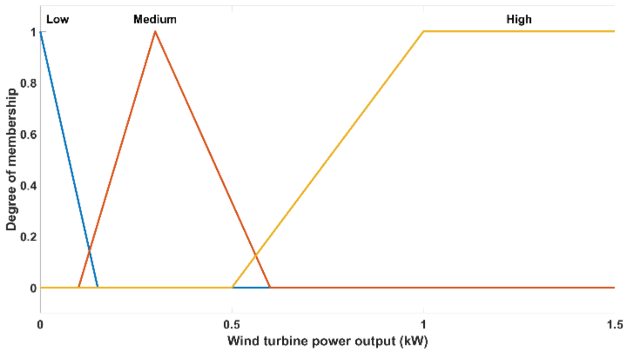


**Fig. 3: Membership function for "Wind Turbine output" fuzzy input variable**

The "controllable consumption" output dynamically manages prioritized load groups labeled P0, P1, P2, and P3, which correspond to household appliance categories defined by their criticality and operational flexibility. Specifically, P0 includes essential appliances for continuous use, such as refrigerators and modems/routers; P1 represents lighting circuits; P2 consists of periodic-use appliances like washing machines and kettles; and P3 covers multimedia or discretionary loads, such as televisions and computers. By interpreting the real-time system state, including renewable generation availability, battery state of charge (SoC), and load demand, the fuzzy controller activates appropriate combinations of these groups. For example, when generation is minimal or the SoC is critically low, only P0 appliances are enabled. Under moderate generation conditions, P0 and P1 are supplied. During surplus generation or when the battery is fully charged, P0, P1, and P3 can be simultaneously activated. The second output variable, "used energy," identifies the preferred energy source or source combination at any given time, which may include the battery, photovoltaic (PV) system, wind turbine (WT), or a hybrid PV + WT contribution.

### 2.2.2. Fuzzy Inference System Design

The fuzzy rule base consists of 14 IF-THEN rules that coordinate inputs to control outputs. Example rules include:

- *If (Electricity consumption is Low), then (Controllable consumption is P0) and (Used energy is Battery).*
- *If (Time of day is Night) and (Wind turbine power output (kW) is Low) and (SOC (%) is Medium) then (Controllable consumption is P0+P1)(Used energy is Battery)*
- *If (Time of day is Early morning) and (Wind turbine power output (kW) is Low) and (Solar panels power output (kW) is Low) and (SOC (%) is High), then (Controllable consumption is P0)(Used energy is Battery) (1).*

These rules are defined to maximize renewable energy use, preserve battery health, and avoid unnecessary load curtailment.

### 2.2.3. Control Architecture Integration

As shown in Fig. 1, the controller operates at the core of the smart home microgrid's energy management system. It receives real-time inputs from PV and wind sources, SoC monitoring, smart meters, and user demand profiles. Outputs from the FIS are used to activate or deactivate specific load categories and to select which

energy source should be dispatched. This ensures optimal matching between generation and demand at any moment.
The control diagram also reflects the advanced load prioritization scheme, highlighting how the controller selects specific combinations like P0+P1+P2 or P0+P1+P3 depending on available energy and load conditions. This hierarchical structure improves operational flexibility, reduces energy wastage, and enhances grid autonomy.

## 3. Results and Discussion

### 3.1. Optimal Microgrid Sizing via Particle Swarm Optimization (PSO)

The Particle Swarm Optimization (PSO) algorithm was employed to determine the optimal configuration of the smart home microgrid under the climatic and demand conditions of Garoua, Cameroon. Based on the optimization results and the standardized component sizes, the system comprises six photovoltaic (PV) panels (totaling 1.59 kW), one wind turbine (rated at 2.0 kW), and a battery bank of approximately 10.63 kWh (equivalent to 3.4 units, each 3.12 kWh).

The economic assessment of this configuration yielded a total annualized cost of $638.05 and a Levelized Cost of Energy (LCOE) of $0.2019/kWh, reflecting a reasonable trade-off between investment and performance for residential use. The cost distribution includes $188.91 for solar panels, $52.88 for the wind turbine, $141.71 for batteries, and $254.56 for the inverter, which is sized at 3.33 kW to accommodate peak load conditions.

In terms of annual energy production, the system generates approximately 6,651 kWh from wind and 3,040 kWh from solar, significantly exceeding the household load demand of 3,159.4 kWh. However, approximately 6,024 kWh of this energy is unused, indicating generation-load mismatch and underutilization of available renewable energy due to storage or demand limitations.

The Loss of Power Supply Probability (LPSP) is calculated at 0.3678, suggesting that the system may not always meet demand, particularly during periods of low generation or high load, without strategic load management. Battery usage statistics show 853.94 kWh charged and 501.87 kWh discharged annually, indicating partial utilization of the storage system.

Fig. 4 illustrates the time-series energy dispatch resulting from the PSO-based optimization of the hybrid PV-WT-Battery system, covering a 5-day (120-hour) horizon. This output represents the baseline system performance, prior to the application of the fuzzy inference system (FIS), and reflects the autonomous operation of the optimally sized system under real-time load and generation variability.

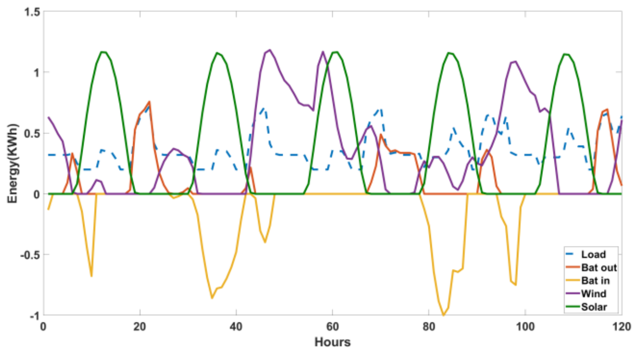


**Fig. 4: Optimized Energy Dispatch from PSO-Based Sizing for Smart Home Microgrid Over 5 Days**

The solar generation profile (green) follows a consistent diurnal pattern, peaking during midday hours, while wind energy production (purple) complements it with stochastic variability, especially during nocturnal hours. The residential load demand (blue dashed line) remains relatively stable, with peak usage during evening hours, representing realistic household consumption patterns.

The battery system’s charge/discharge behavior is shown through the orange (“Bat out”) and yellow (“Bat in”) curves. Energy storage is activated during surplus generation periods (typically midday solar excess), and discharged during energy deficits, effectively smoothing the supply-demand profile. This highlights the battery's role in ensuring continuous load supply and mitigating curtailment.

The PSO optimization ensures proper sizing and coordinated operation of system components, resulting in minimal excess energy and no loss of power supply. These optimized dispatch patterns are then used as inputs to the fuzzy inference system (FIS), which introduces intelligent demand-side management by adjusting the controllable loads according to source availability and battery SoC.

In summary, the figure validates the effectiveness of the PSO algorithm in producing a feasible and economically viable dispatch strategy that serves as a robust input for the subsequent DR-FIS controller implementation.

Regarding the optimization approach, Fig. 5 presents the convergence behavior of the Particle Swarm Optimization (PSO) algorithm during the optimal sizing of the smart home hybrid microgrid system. The vertical axis shows the fitness function value, which aggregates cost, reliability, and efficiency metrics, while the horizontal axis indicates the number of iterations (up to 50).

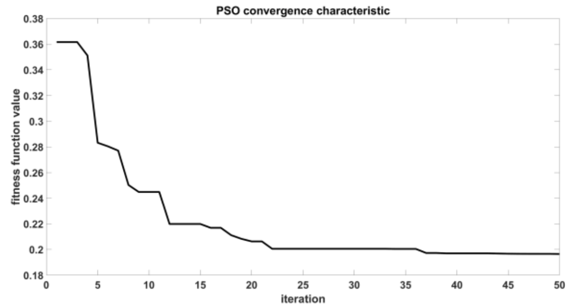


**Fig. 5: PSO Convergence Curve for Multi-Objective Microgrid Sizing**

The algorithm exhibits a steep descent in the early iterations (1–10), indicating rapid improvement in solution quality as particles explore the search space. This is characteristic of the global exploration phase of PSO, where diverse particle positions allow the swarm to broadly sample the decision space.

From iteration 10 onward, the curve transitions into a more gradual decline, indicating that the swarm has narrowed in on a promising region of the solution space. By iteration 25, the fitness function stabilizes around 0.20, with marginal improvements in subsequent iterations. This plateau signals the convergence phase, where particles oscillate near the global optimum, with little variation in velocity or position.

The rapid early convergence and eventual stabilization demonstrate the efficiency and robustness of PSO in identifying an optimal or near-optimal configuration of the microgrid components (PV, WT, and battery capacities). The convergence behavior also implies computational efficiency, as acceptable results are obtained within a limited number of iterations, making this optimization technique suitable for real-time or iterative design applications in smart energy systems.

While the optimal component sizing establishes the physical capabilities of the microgrid, dynamic energy management is required to prioritize loads and improve energy use efficiency. This is addressed in the following section using a fuzzy logic-based controller.

## *3.2. Demand Response-Based Energy Management using Fuzzy Inference System (FIS)*

This subsection focuses on the post-sizing operational optimization using the fuzzy controller for smart load prioritization and energy dispatch.

In this study, a fuzzy logic-based Demand Response (DR) controller was implemented to manage energy use within a smart home microgrid. The Fuzzy Inference System (FIS) dynamically adjusts controllable loads based on the state of charge (SoC) of the battery, and the real-time outputs of the photovoltaic (PV) and wind turbine (WT) subsystems, energy demand, and time of the day.

Fig. 6 illustrates how controllable loads are grouped into sets (P0 to P0+P2+P3) using fuzzy linguistic variables. Each set corresponds to specific household appliances with different priority levels. Similarly, Fig.

7 maps the possible energy sources to fuzzy output values, ranging from 1 (Battery) to 4 (PV + WT). These membership functions enable smooth transitions and decision-making under uncertainty. The fuzzy rules combine the five inputs to determine both the load activation level and energy source. For example, representing rule 2, if *Time = Night, WT output = Low, SOC = Medium, then activate P0+P1 using Battery*.

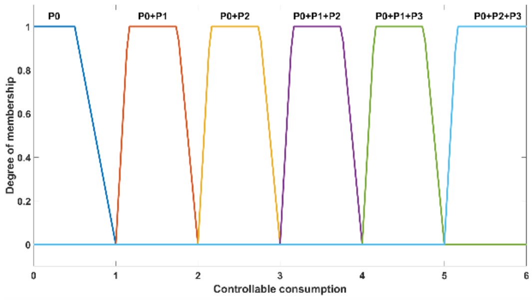


**Fig. 6: Membership functions for controllable consumption output**

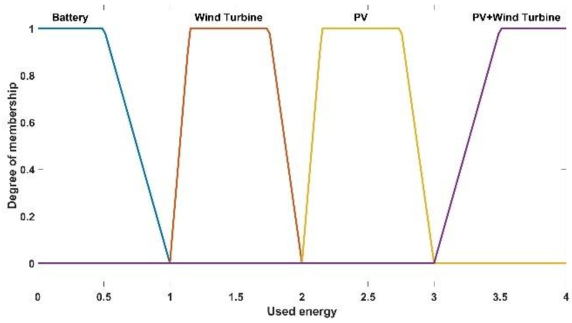


**Fig. 7: Membership functions for used energy output**

Fig. 8 presents the dynamic output of the fuzzy controller during a 120-hour simulation. The blue curve shows the activated controllable loads, while the orange curve shows the selected energy source.

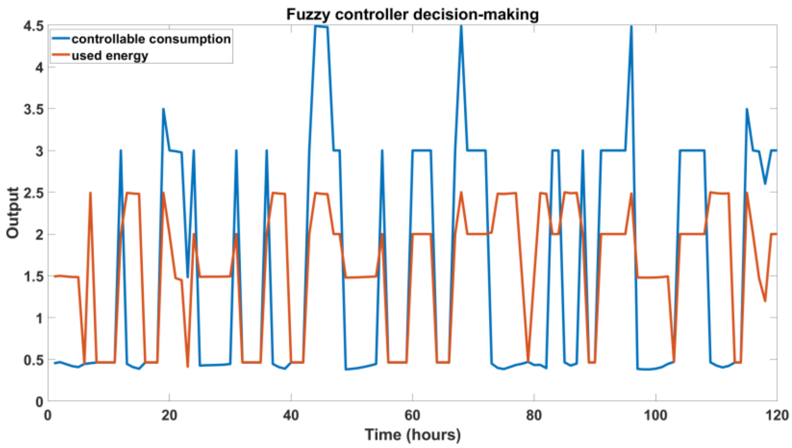


**Fig. 8: Time-series of fuzzy controller decision-making: controllable consumption and used energy source**

Key insights include:

- During peak PV and WT generation, the controller permits higher consumption levels (e.g., output > 3).
- In times of energy scarcity or low SoC, consumption is restricted to essential loads (e.g., output = 0.5–1.5) and the battery is preferred.

Fig. 9 reveals how the controllable consumption depends on the battery's state of charge and the wind turbine power.

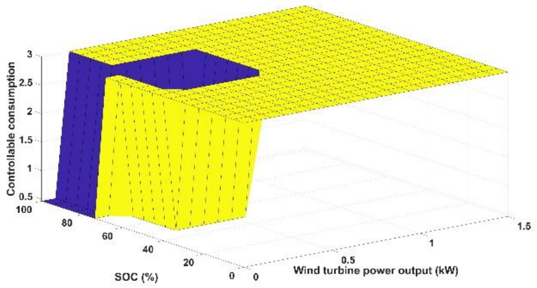


**Fig. 9: 3D surface plot of controllable consumption vs. SoC and WT output**

The controllable-consumption output increases stepwise from P0 to P0+P2 to P0+P1+P2 as SoC and WT power improve. A threshold near SoC ≈ 60 % enables lighting (P1) in addition to essentials and periodic loads, while low SoC restricts consumption (often to P0). In this slice, P3 loads are never authorized, indicating the controller's conservative stance in the absence of a clear renewable surplus.

Finally, energy management within the microgrid system is governed by a demand response (DR) controller based on fuzzy logic, as illustrated in fig. 10. This figure presents a comparison between the real consumption profile (in red) and the fuzzy-managed consumption profile (in blue) over a 120-hour simulation period. By dynamically adjusting controllable loads in real time, considering available renewable energy, state-of-charge (SOC), energy demand, and time of day, the fuzzy controller effectively flattens load peaks and fills demand valleys.

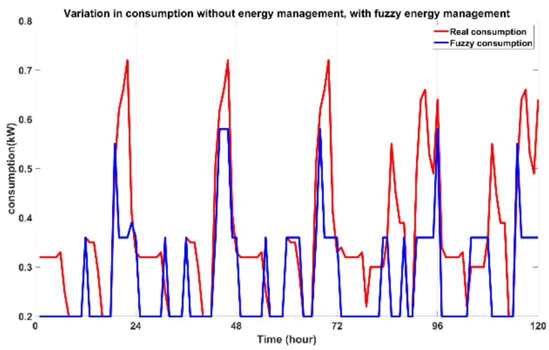


**Fig. 10: variation in consumption without and with fuzzy energy management**

This results in an 8.675% reduction in total energy consumption, achieved through strategic load deferral and prioritization. Such performance underscores the system's ability to enhance energy efficiency and demand-side flexibility without compromising user comfort. Moreover, the fuzzy logic controller ensures that renewable energy production is prioritized. Despite the consumption optimization, approximately 15.0676% of the generated renewable energy remains unutilized by the household and is instead exported back to the grid. This surplus, originating from photovoltaic and wind sources, contributes to improved system economics by creating an opportunity for financial return through energy sales, particularly under feed-in tariff or net metering schemes. Beyond direct grid export, the excess renewable energy can also be stored for later use or redirected to support secondary applications, such as hydrogen production or thermal energy storage, thereby enhancing the overall value, flexibility, and resilience of the microgrid system.

## 4. Conclusions

This work highlights the effectiveness of integrating fuzzy logic-based demand response into smart home microgrids powered by hybrid renewable energy. The Mamdani Fuzzy Inference System (FIS) successfully utilizes real-time inputs, such as PV and WT outputs, battery SoC, consumption level, and time of day, to make adaptive decisions about controllable load activation and energy source prioritization. The system not only improves energy use efficiency by reducing consumption by 8.675%, but also allows strategic load shifting that aligns with renewable availability, thereby reducing stress on the battery system and flattening demand peaks. Moreover, with 15.0676% of generated energy exported to the grid, the microgrid presents opportunities for revenue generation and supports grid decarbonization through surplus renewable integration. The hybrid PV-WT-battery configuration optimized via PSO ensures both technical reliability and economic feasibility, making this approach practical for real-world applications in resource-constrained environments like Cameroon.

The results reinforce the potential of fuzzy logic controllers in real-time energy management, especially when integrated into optimized renewable microgrids. Future research could explore the integration of secondary applications such as hydrogen production or thermal energy storage, and the incorporation of user behavior models for further personalization and efficiency improvements.

## 5. References

Acun, F., & Çunkaş, M. (2023). Low - cost fuzzy logic - controlled home energy management system. *Journal of Electrical Systems and Information Technology*. https://doi.org/10.1186/s43067-023-00100-6

Ain, Q., Iqbal, S., & Khan, S. A. (2018). *IoT Operating System Based Fuzzy Inference System for Home Energy Management System in Smart Buildings*. 1–30. https://doi.org/10.3390/s18092802

Alshammari, N., & Asumadu, J. (2020). Optimum unit sizing of hybrid renewable energy system utilizing harmony search , Jaya and particle swarm optimization algorithms. *Sustainable Cities and Society*, *60*(November 2019), 102255. https://doi.org/10.1016/j.scs.2020.102255

Barakat, S., Ibrahim, H., & Elbaset, A. A. (2020). Multi-objective optimization of grid-connected PV-wind hybrid system considering reliability, cost, and environmental aspects. *Sustainable Cities and Society*, *60*, 102178. https://doi.org/10.1016/j.scs.2020.102178

Beheshtikhoo, A., Pourgholi, M., & Khazaee, I. (2023). Design of type-2 fuzzy logic controller in a smart home energy management system with a combination of renewable energy and an electric vehicle. *Journal of Building Engineering*, *68*(July 2022), 106097. https://doi.org/10.1016/j.jobe.2023.106097

Bukar, A. L., Tan, C. W., & Lau, K. Y. (2019). Optimal sizing of an autonomous photovoltaic/wind/battery/diesel generator microgrid using grasshopper optimization algorithm. *Solar Energy*, *188*(March), 685–696. https://doi.org/10.1016/j.solener.2019.06.050

Hermann, D. T., Franck Armel, T. K., René, T., & Donatien, N. (2021). Consideration of some optimization techniques to design a hybrid energy system for a building in Cameroon. *Energy and Built Environment*, *January*. https://doi.org/10.1016/j.enbenv.2021.01.007

Javaid, S., Javaid, N., Alhussein, M., Aurangzeb, K., Iqbal, S., & Anwar, M. S. (2023). Towards efficient human – machine interaction for home energy management with seasonal scheduling using deep fuzzy neural optimizer. *Cognition, Technology & Work*, *25*(2), 291–304. https://doi.org/10.1007/s10111-023-00728-4

Kotb, K. M., Elkadeem, M. R., Elmorshedy, M. F., & Dán, A. (2020). Coordinated power management and optimized techno-enviro-economic design of an autonomous hybrid renewable microgrid: A case study in Egypt. *Energy Conversion and Management*, *221*(July), 113185. https://doi.org/10.1016/j.enconman.2020.113185

Ma, T., & Javed, M. S. (2019). Integrated sizing of hybrid PV-wind-battery system for remote island considering the saturation of each renewable energy resource. *Energy Conversion and Management*, *182*(October 2018), 178–190. https://doi.org/10.1016/j.enconman.2018.12.059

Paramathma, M. K., Devaraj, D., Selvi, V. A. I., Karuppasamypandian, M., Nagar, A., & Nadu, T. (2021). *Development of Fuzzy Logic Based Approach for Consumer Side Management in Smart Home*. 1056–1061.

Ramli, M. A. M., Bouchekara, H. R. E. H., & Alghamdi, A. S. (2018). Optimal sizing of PV/wind/diesel hybrid microgrid system using multi-objective self-adaptive differential evolution algorithm. *Renewable Energy*, *121*, 400–411. https://doi.org/10.1016/j.renene.2018.01.058

Tezer, T., Yaman, R., & Yaman, G. (2017). Evaluation of approaches used for optimization of stand-alone hybrid renewable energy systems. *Renewable and Sustainable Energy Reviews*, *73*(December 2016), 840–853. https://doi.org/10.1016/j.rser.2017.01.118

Zaki Diab, A. A., Sultan, H. M., Mohamed, I. S., Kuznetsov Oleg, N., & Do, T. D. (2019). Application of different optimization algorithms for optimal sizing of pv/wind/diesel/battery storage stand-alone hybrid microgrid. *IEEE Access*, *7*, 119223–119245. https://doi.org/10.1109/ACCESS.2019.2936656

Žarković, M., & Dobrić, G. (2019). *Fuzzy expert system for management of smart hybrid energy microgrid Fuzzy expert system for management of smart hybrid energy microgrid*. *034101*(April). https://doi.org/10.1063/1.5097564